Supplementary Material (ESI) for PCCP

Density functional study of structural and electronic properties of bimetallic copper–gold clusters: comparison with pure and doped gold clusters

Supplementary Information

Huai-Qian Wang,[a] Xiao-Yu Kuang, [a,b,*] Hui-Fang Li [a]

[a] Institute of Atomic and Molecular Physics, Sichuan University, Chengdu 610065, China

[b]International Centre for Materials Physics, Academia Sinica, Shenyang 110016, China

1. Supplementary calculated results using three different functionals.

In the following, we present more detailed geometrical structure and relative energies between the energetically lowest structures for $Au_{n-1}Cu^{\lambda}$ ($\lambda = 0, +1, -1$; $2 \le n \le 9$) using three different DFT calculations (BPW91, BP86 and B3LYP), these results underline that the geometries of all the clusters obtained within the three functionals are similar, although the order of isomers is reversed in some cases. From Table 1, it can be seen that for the $Au_{n-1}Cu$ cluster ($2 \le n \le 9$), the ground state structures predicted by the BP86 and BPW91 methods are consistent with those predicted by B3LYP method. In the case of n=7 and 9, the energies of 7-N-c and 9-N-c predicted by B3LYP method are lower than those of 7-N-d and 9-N-d by 0.005 and 0.031eV, respectively, while the BP86 and BPW91 methods predict 7-N-c and 9-N-c to lie slightly higher than 7-N-d and 9-N-d by 0.01, 0.004 eV (BP86) and 0.032, 0.03 eV (BPW91). For the $Au_{n-1}Cu^{+}$ cluster the only difference of the geometrical structure among the three functionals is that BP86 and BPW91 predicte 9-C-b to lie higher than 9-C-c by 0.013 and 0.033 eV, respectively (see Table S2). The geometries of the $Au_{n-1}Cu$ cluster anions calculated by BP86 and BPW91 functionals are also essentially similar to those obtained by B3LYP functional except for n=8. The ground state structure is either a C_s structure 8-A-a or a C_1 structure 8-A-b, depending on the theoretical method. The B3LYP method predicts 8-A-a to lie lower in energy than 8-A-b by 0.023 eV, while the BP86 and BPW91 methods predict 8-A-a to lie higher than 8-A-b by 0.059 and 0.050 eV, respectively. Thus structures 8-A-a and 8-A-b are essentially degenerate in energy. In addition, structure 6-A-b is predicted to be lower than 6-A-c by the B3LYP and BPW91 methods, while it is predicted by the BP86 method to lie above structure 6-A-c by 0.006 eV. The order of structures 7-A-b and 7-A-c predicted by the B3LYP is consistent with that predicted by BP86, but contrary to the result of BPW91. The corresponding results are listed in Table S3.

It can be seen from Tables S1-S3 that although the B3LYP results give small

relative energies than by the BPW91 and BP86 functionals systemically, they show very similar geometries and the other features. This suggests that geometries of all the clusters should be correctly predicted by all functionals.

Table S1. Geometries (Geo), symmetries (sym), electron states, and relative energies (in eV) between the energetically lowest structures for $Au_{n-1}Cu$ ($2 \le n \le 9$), optimized at the different methods.

Geo	B3LYP			BP86			BPW9		
	Sym	State	RE(eV)	Sym	State	RE(eV)	Sym	State	RE(eV)
3-N-a	C_{2v}	$^2B_2$	0	C_{2v}	$^2B_2$	0	C_{2v}	$^2B_2$	0
3-N-b	C_s	$^2A'$	0.348	C_s	$^2A'$	0.414	C_s	$^2A'$	0.409
4-N-a	C_s	$^1A'$	0	C_s	$^1A'$	0	C_s	$^1A'$	0
4-N-b	C_s	$^1A'$	0.143	C_s	$^1A'$	0.205	C_s	$^1A'$	0.198
4-N-c	C_s	$^1A'$	0.863	C_s	$^1A'$	0.949	C_s	$^1A'$	0.948
5-N-a	C_{2v}	$^2A_1$	0	C_{2v}	$^2A_1$	0	C_{2v}	$^2A_1$	0
5-N-b	C_s	$^2A'$	0.127	C_s	$^2A'$	0.138	C_s	$^2A'$	0.143
5-N-c	C_s	$^2A'$	0.817	C_s	$^2A'$	0.952	C_s	$^2A'$	0.937
6-N-a	C_{2v}	$^1A_1$	0	C_{2v}	$^1A_1$	0	C_{2v}	$^1A_1$	0
6-N-b	C_s	$^1A'$	0.430	C_s	$^1A'$	0.400	C_s	$^1A'$	0.409
6-N-c	C_{2v}	$^1A_1$	0.625	C_{2v}	$^1A_1$	0.622	C_{2v}	$^1A_1$	0.639
6-N-d	C_s	$^1A'$	2.041	C_s	$^1A'$	2.156	C_s	$^1A'$	2.150
7-N-a	C_1	^2A	0	C_1	^2A	0	C_1	^2A	0
7-N-b	C_s	$^2A'$	0.297	C_s	$^2A'$	0.309	C_s	$^2A'$	0.320
7-N-c	C_1	^2A	0.590	C_1	^2A	0.629	C_1	^2A	0.644
7-N-d	C_s	$^2A'$	0.595	C_s	$^2A'$	0.619	C_s	$^2A'$	0.640
8-N-a	C_1	^1A	0	C_1	^1A	0	C_1	^1A	0
8-N-b	C_1	^1A	0.353	C_1	^1A	0.201	C_1	^1A	0.216
8-N-c	C_s	$^1A'$	0.410	C_s	$^1A'$	0.242	C_s	$^1A'$	0.268
8-N-d	C_s	$^1A'$	0.496	C_s	$^1A'$	0.493	C_s	$^1A'$	0.516
9-N-a	C_{2v}	$^2A_1$	0	C_{2v}	$^2A_1$	0	C_{2v}	$^2A_1$	0
9-N-b	C_{2v}	$^2A_1$	0.182	C_{2v}	$^2A_1$	0.157	C_{2v}	$^2A_1$	0.156
9-N-c	C_1	^2A	0.248	C_1	^2A	0.169	C_1	^2A	0.173
9-N-d	C_1	^2A	0.279	C_1	^2A	0.137	C_1	^2A	0.143

Table S2. Geometries (Geo), symmetries (sym), electron states, and relative energies (in eV) between the energetically lowest structures for $Au_{n-1}Cu^{+}$ ($2 \le n \le 9$), optimized at the different methods.

Geo	B3LYP			BP86			BPW91		
	Sym	State	RE(eV)	Sym	State	RE(eV)	Sym	State	RE(eV)
4-C-a	C_{2v}	$^2B_2$	0	C_{2v}	$^2B_2$	0	C_{2v}	$^2B_2$	0
4-C-b	C_s	$^2A'$	0.202	C_s	$^2A'$	0.271	C_s	$^2A'$	0.262
4-C-c	C_{2v}	$^2A_1$	0.343	C_{2v}	$^2A_1$	0.376	C_{2v}	$^2A_1$	0.378
5-C-a	C_s	$^1A'$	0	C_s	$^1A'$	0	C_s	$^1A'$	0
5-C-b	C_2	^1A	0.053	C_2	^1A	0.086	C_2	^1A	0.063
6-C-a	C_s	$^2A'$	0	C_s	$^2A'$	0	C_s	$^2A'$	0
6-C-b	C_1	^2A	0.011	C_1	^2A	0.059	C_1	^2A	0.058
6-C-c	C_1	^2A	0.058	C_1	^2A	0.199	C_1	^2A	0.194
6-C-d	C_s	$^2A'$	0.138	C_s	$^2A'$	0.316	C_s	$^2A'$	0.320
7-C-a	C_1	^1A	0	C_1	^1A	0	C_1	^1A	0
7-C-b	C_1	^1A	0.210	C_1	^1A	0.250	C_1	^1A	0.236
7-C-c	C_2	^1A	0.220	C_2	^1A	0.299	C_2	^1A	0.289
7-C-d	C_s	$^1A'$	0.259	C_s	$^1A'$	0.349	C_s	$^1A'$	0.354
8-C-a	C_1	^2A	0	C_1	^2A	0	C_1	^2A	0
8-C-b	C_1	^2A	0.160	C_1	^2A	0.185	C_1	^2A	0.176
8-C-c	C_{2v}	$^2B_2$	0.325	C_{2v}	$^2B_2$	0.361	C_{2v}	$^2B_2$	0.359
8-C-d	C_s	$^2A'$	0.443	C_s	$^2A'$	0.539	C_s	$^2A'$	0.550
9-C-a	C_{2v}	$^1A_1$	0	C_{2v}	$^1A_1$	0	C_{2v}	$^1A_1$	0
9-C-b	C_s	$^1A'$	0.644	C_s	$^1A'$	0.668	C_s	$^1A'$	0.695
9-C-c	C_1	^1A	0.757	C_s	$^1A'$	0.655	C_s	$^1A'$	0.662
9-C-d	C_1	^1A	1.526	C_1	^1A	1.467	C_1	^1A	1.471

Table S3. Geometries (Geo), symmetries (sym), electron states, and relative energies (in eV) between the energetically lowest structures for $Au_{n-1}Cu^-$ ($2 \le n \le 9$), optimized at the different methods.

Geo	B3LYP			BP86			BPW91		
	Sym	State	RE(eV)	Sym	State	RE(eV)	Sym	State	RE(eV)
3-A-a	$D_{\infty h}$	$^1\Sigma_g$	0	$D_{\infty h}$	$^1\Sigma_g$	0	$D_{\infty h}$	$^1\Sigma_g$	0
3-A-b	$C_{\infty v}$	$^1\Sigma$	0.802	$C_{\infty v}$	$^1\Sigma$	0.781	$C_{\infty v}$	$^1\Sigma$	0.793
4-A-a	C_s	$^2A'$	0	C_s	$^2A'$	0	C_s	$^2A'$	0
4-A-b	C_{2v}	$^2A_1$	0.255	C_{2v}	$^2A_1$	0.198	C_{2v}	$^2A_1$	0.214
4-A-c	C_s	$^2A'$	0.560	C_s	$^2A'$	0.539	C_s	$^2A'$	0.541
4-A-d	$C_{\infty v}$	$^2\Sigma$	0.652	C_s	$^2A'$	0.745	C_s	$^2A'$	0.741
4-A-e	C_s	$^2A'$	0.925	C_s	$^2A'$	0.962	C_s	$^2A'$	0.977
5-A-a	C_{2v}	$^1A_1$	0	C_{2v}	$^1A_1$	0	C_{2v}	$^1A_1$	0
5-A-b	C_s	$^1A'$	0.109	C_s	$^1A'$	0.179	C_s	$^1A'$	0.160
5-A-c	C_s	$^1A'$	0.333	C_s	$^1A'$	0.469	C_s	$^1A'$	0.446
5-A-d	C_s	$^1A'$	0.733	C_s	$^1A'$	0.924	C_s	$^1A'$	0.910
6-A-a	C_{2v}	$^2A_1$	0	C_{2v}	$^2A_1$	0	C_{2v}	$^2A_1$	0
6-A-b	C_{2v}	$^2B_2$	0.456	C_{2v}	$^2B_2$	0.586	C_{2v}	$^2B_2$	0.573
6-A-c	C_1	^2A	0.620	C_1	^2A	0.580	C_1	^2A	0.579
6-A-d	C_{2v}	$^2A_1$	0.840	C_{2v}	$^2A_1$	0.849	C_{2v}	$^2A_1$	0.865
6-A-e	C_s	$^2A'$	1.192	C_s	$^2A'$	1.373	C_s	$^2A'$	1.371
7-A-a	C_1	^1A	0	C_1	^1A	0	C_1	^1A	0
7-A-b	C_2	^1A	0.249	C_1	^1A	0.030	C_1	^1A	0.443
7-A-c	C_s	$^1A'$	0.368	C_s	$^1A'$	0.358	C_s	$^1A'$	0.365
7-A-d	C_s	$^1A'$	0.670	C_s	$^1A'$	0.661	C_s	$^1A'$	0.684
7-A-e	C_1	^1A	0.982	C_1	^1A	0.973	C_1	^1A	0.993
8-A-a	C_s	$^2A'$	0	C_s	$^2A'$	0.059	C_s	$^2A'$	0.050
8-A-b	C_1	^2A	0.023	C_1	^2A	0	C_1	^2A	0
8-A-c	C_s	$^2A'$	0.580	C_s	$^2A'$	0.510	C_s	$^2A'$	0.522
8-A-d	C_s	$^2A'$	0.729	C_s	$^2A'$	0.773	C_s	$^2A'$	0.780
9-A-a	C_s	$^1A'$	0	C_1	^1A	0	C_1	^1A	0
9-A-b	C_{2v}	$^1A_1$	0.136	C_{2v}	$^1A_1$	0.130	C_{2v}	$^1A_1$	0.141
9-A-c	C_{2v}	$^1A_1$	0.820	C_{2v}	$^1A_1$	0.738	C_2	^1A	0.746
9-A-d	C_s	$^1A'$	1.035	C_s	$^1A'$	0.805	C_s	$^1A'$	0.828

2. Structural and energetic characteristics of the lowest-energy isomers as a function of size for doped and bare gold clusters.

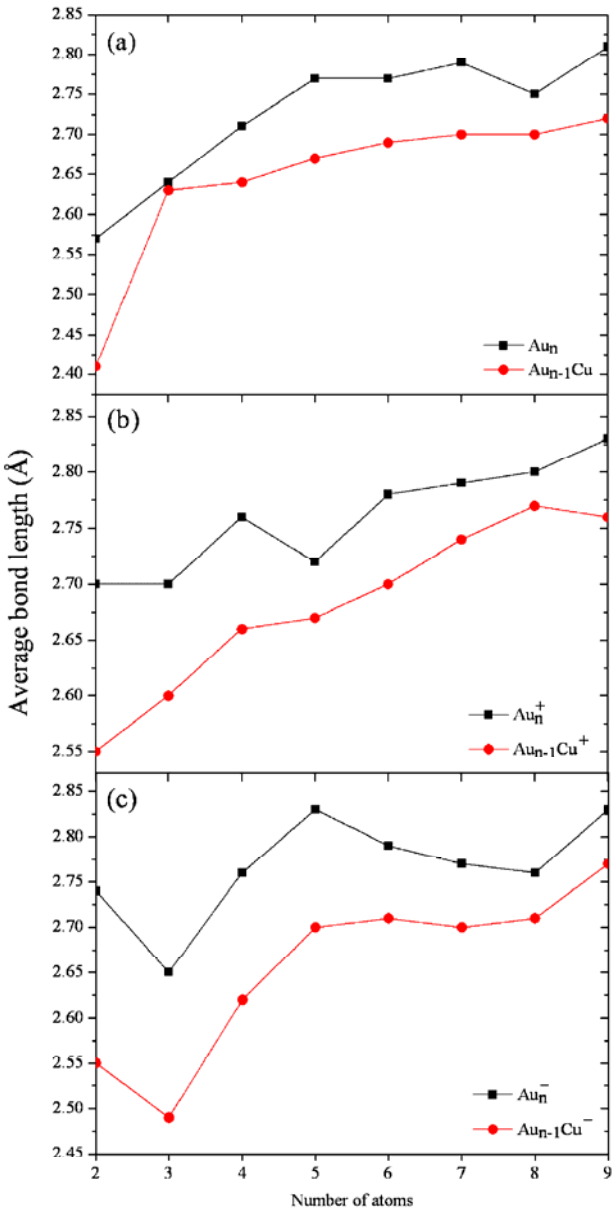

Figure S1. Average nearest-neighbor distance of the lowest-energy isomers as a function of size for $Au_{n-1}Cu^{\lambda}$ (charge $\lambda = 0, \pm 1$; $2 \le n \le 9$) clusters as well as their corresponding bare gold clusters. (a), (b), and (c) correspond to neutral ($\lambda = 0$), cationic ($\lambda = +1$), and anionic ($\lambda = -1$) species, respectively.

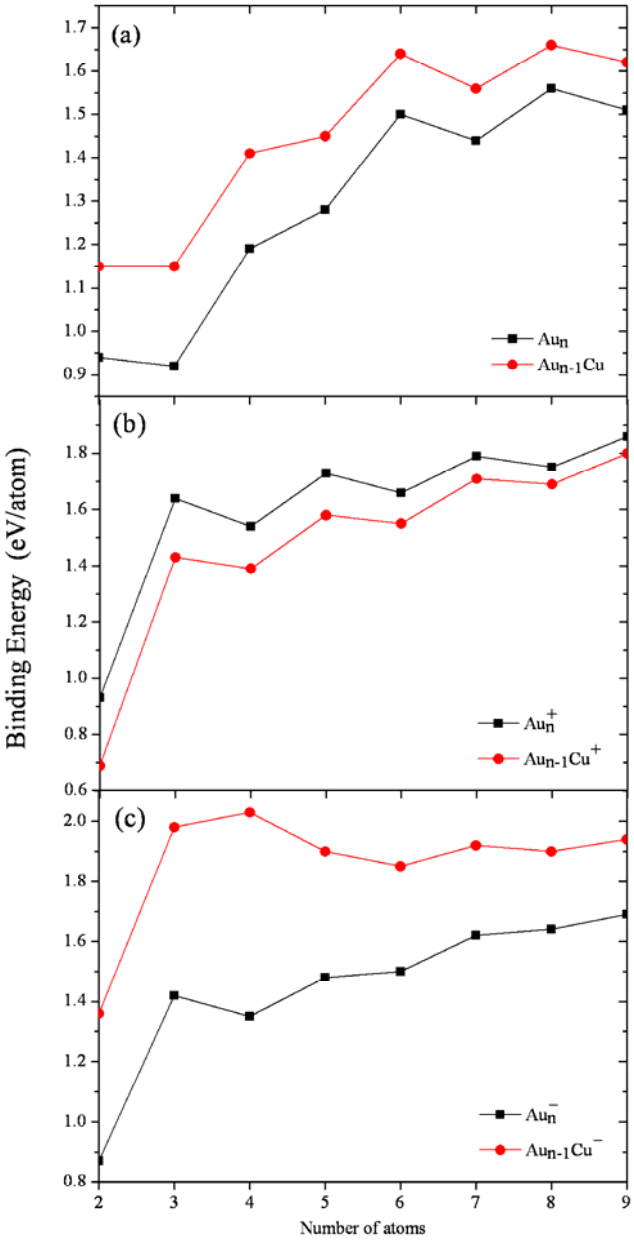

Figure S2. The calculated binding energy per atom of neutral and charged clusters ($Au_{n-1}Cu^{\lambda}$ and Au_n^{λ} (charge $\lambda = 0, \pm 1; 2 \le n \le 9$)) is represented versus the number of atoms. (a), (b), and (c) correspond to neutral ($\lambda = 0$), cationic ($\lambda = +1$), and anionic ($\lambda = -1$) species, respectively.

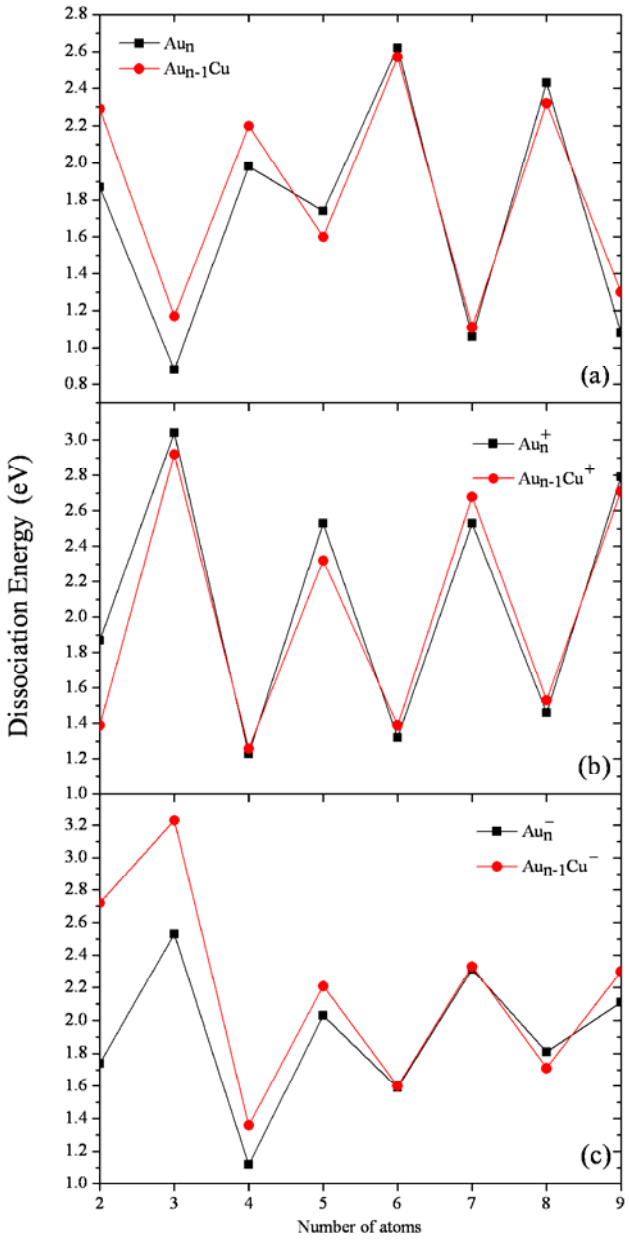

Figure S3. Size dependence of dissociation energies for the lowest structures of $Au_{n-1}Cu^{\lambda}$ and Au_n^{λ} (charge $\lambda = 0, \pm 1; 2 \le n \le 9$).

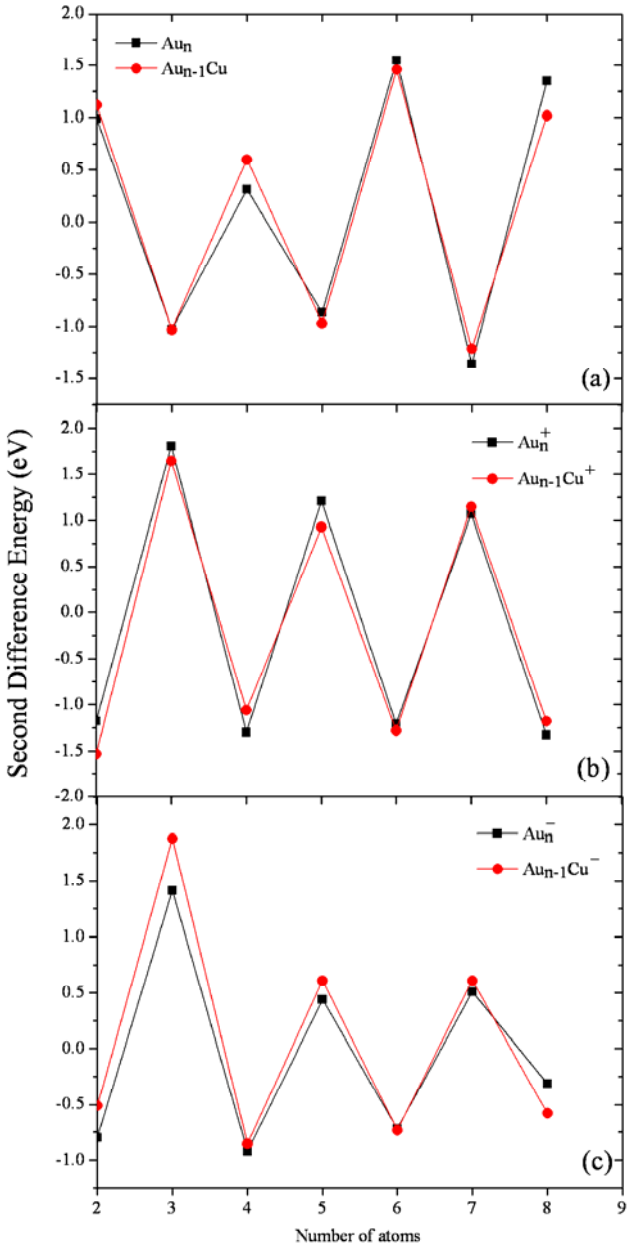

Figure S4. Second total energy differences versus number of atoms for neutral, anionic, and cationic clusters of the lowest-energy structure of $Au_{n-1}Cu^{\lambda}$ and Au_n^{λ} (charge $\lambda = 0, \pm 1; 2 \le n \le 9$) clusters. (a), (b), and (c) correspond to neutral ($\lambda = 0$), cationic ($\lambda = +1$), and anionic ($\lambda = -1$) species, respectively.